

Research Article

A Wide-Band Test Fixture for Analyzing Parasitic Effects of RF Passive SMD Components

Xin Cao and Zongxi Tang

School of Electronic Engineering, University of Electronic Science and Technology of China, No. 2006, Xiyuan Road, West Hi-Tech Zone, Chengdu 611731, China

Correspondence should be addressed to Xin Cao; 798899759@qq.com

Received 18 February 2017; Accepted 27 April 2017; Published 14 May 2017

Academic Editor: N. Nasimuddin

Copyright © 2017 Xin Cao and Zongxi Tang. This is an open access article distributed under the Creative Commons Attribution License, which permits unrestricted use, distribution, and reproduction in any medium, provided the original work is properly cited.

A wide-band test fixture is designed for the measurement of parasitic effects of RF passive SMD (surface mounted devices) components. Two calibration methods, TRM (Thru-Reflect-Match) from 45 MHz to 2 GHz and TRL (Thru-Reflect-Line) from 2 GHz to 12 GHz, are used for error correction. The measurement standards and fixture are designed based on these two calibration methods. For experimental verification, the multilayered ceramic SMD capacitors of Johanson Technology are measured. The parasitic effects of the SMD capacitors are analyzed. The designed fixture is feasible and applicable for quick and accurate measurement of RF passive SMD components.

1. Introduction

With the development of electronic technology, SMD components have been widely used in the design of microwave circuits and wireless communication systems. Therefore, studying the SMD component measurement methods and extracting accurate high-frequency component characteristic parameters in high frequency are very important. However, for conventional SOLT (Short-Open-Load-Thru) calibration method, with the increase of the operating frequency, the parasitic effects caused by the calibration standards increase, especially by the fringing capacitance of the open standard. The fringing effect of open standard can be adjusted by using EM modeling and inputting the model value into the VNA. For TRL (Thru-Reflect-Line) calibration method, the calibration bandwidth is limited by the line standard due to the line phase ambiguity, where the eigenvalue matrix becomes unitary and can cause measurement inaccuracy, if only one LINE is used [1, 2]. The bandwidth can be extended using multiple LINES instead of one LINE. In our paper, TRM (Thru-Reflect-Match) calibration is introduced at low frequency range to avoid phase ambiguity. Then, based on the theoretical analysis, the measurement fixture is designed.

Parasitic effects of SMD capacitors are analyzed. Excellent results are achieved.

2. Theory, Analysis, and Results

TRL calibration is based on the ten-term error model (shown in Figure 1). Based on the calculation using Mason formula, the relationship between the measured S-parameters and actual S-parameters of the network can be expressed as [3]

$$\begin{aligned} S'_{11} &= e_{00} \\ &+ \frac{e_{10}e_{01}S_{11}(1 - S_{22}e_{22}) + e_{10}e_{01}S_{21}S_{12}e_{22}}{1 - S_{11}e_{11} - S_{22}e_{22} - S_{21}S_{12}e_{11}e_{22} + S_{11}S_{22}e_{11}e_{22}} \\ S'_{21} &= e_{30} \\ &+ \frac{e_{10}e_{32}S_{21}}{1 - S_{11}e_{11} - S_{22}e_{22} - S_{21}S_{12}e_{11}e_{22} + S_{11}S_{22}e_{11}e_{22}} \end{aligned}$$

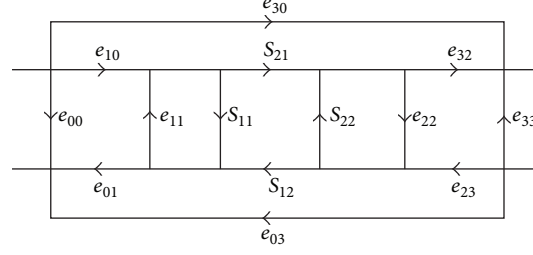


FIGURE 1: The ten-term error model of a two-port network.

$$\begin{aligned}
 S'_{12} &= e_{03} \\
 &+ \frac{e_{01}e_{23}S_{12}}{1 - S_{11}e_{11} - S_{22}e_{22} - S_{21}S_{12}e_{11}e_{22} + S_{11}S_{22}e_{11}e_{22}} \\
 S'_{22} &= e_{33} \\
 &+ \frac{e_{23}e_{32}S_{22}(1 - S_{11}e_{11}) + e_{23}e_{32}S_{21}S_{12}e_{11}}{1 - S_{11}e_{11} - S_{22}e_{22} - S_{21}S_{12}e_{11}e_{22} + S_{11}S_{22}e_{11}e_{22}}. \quad (1)
 \end{aligned}$$

For reflection calibration, the reflect standards (open-circuited or short-circuited) are connected to the measurement ports. The reflection coefficient is Γ_R . Then, $S_{21} = S_{12} = 0$ and $S_{11} = S_{22} = \Gamma_R$. The measured values for reflect standard are

$$\begin{aligned}
 S_{11R} &= e_{00} + \frac{e_{10}e_{01}\Gamma_R}{1 - e_{11}\Gamma_R} \\
 S_{21R} &= e_{30} \\
 S_{22R} &= e_{33} + \frac{e_{23}e_{32}\Gamma_R}{1 - e_{22}\Gamma_R} \\
 S_{12R} &= e_{03}. \quad (2)
 \end{aligned}$$

For the thru calibration, it can be regarded as connecting a central network with $S_{21} = S_{12} = 1$ and $S_{11} = S_{22} = 0$. Then, the measured values for thru standard are

$$\begin{aligned}
 S_{11T} &= e_{00} + \frac{e_{10}e_{01}e_{22}}{1 - e_{11}e_{22}} \\
 S_{21T} &= e_{30} + \frac{e_{10}e_{32}}{1 - e_{11}e_{22}} \\
 S_{22T} &= e_{33} + \frac{e_{23}e_{32}e_{11}}{1 - e_{11}e_{22}} \\
 S_{12T} &= e_{03} + \frac{e_{23}e_{01}}{1 - e_{11}e_{22}}. \quad (3)
 \end{aligned}$$

The last one is line calibration. A segment of 50Ω transmission line with the electrical length l is connected to the ports.

The S-parameters of the line standard are $S_{11} = S_{22} = 0$ and $S_{12} = S_{21} = e^{-j\beta l}$, and then the corresponding measured values can be given as

$$\begin{aligned}
 S_{11L} &= e_{00} + \frac{e_{10}e_{01}e_{22}e^{-j2\beta l}}{1 - e_{11}e_{22}e^{-j2\beta l}} \\
 S_{21L} &= e_{30} + \frac{e_{10}e_{32}e^{-j2\beta l}}{1 - e_{11}e_{22}e^{-j2\beta l}} \\
 S_{22L} &= e_{33} + \frac{e_{23}e_{32}e_{11}e^{-j2\beta l}}{1 - e_{11}e_{22}e^{-j2\beta l}} \\
 S_{12L} &= e_{03} + \frac{e_{23}e_{01}e^{-j2\beta l}}{1 - e_{11}e_{22}e^{-j2\beta l}}. \quad (4)
 \end{aligned}$$

Besides the ten error terms, the reflection coefficient Γ_R of the reflect standard and the phase constant β of the line standard are also unknown. So, there are total twelve unknown factors, which can be solved by the twelve equations: (2)–(4). The line standard provides the key attributes to generate a good calibration. One critical factor of the line standard is that its length should be different from the length of the thru standard, so that the phase shift of the line standard is different from that of the thru standard by at least 20° and no more than 160° . If the phase differences of these two standards get close to 0° or 180° , the inaccuracy of calibration will be magnified enormously due to potential singular points in equation solving. Therefore, the frequency ratio for TRL calibration method should not exceed 1:6. Our design is to widen the bandwidth with no cost of measurement accuracy; therefore TRM calibration method is adopted at low frequency range. Since two unknown factors β and l can easily be eliminated, the measured values for match standards are

$$\begin{aligned}
 S_{11M} &= e_{00} \\
 S_{22M} &= e_{33}. \quad (5)
 \end{aligned}$$

Then the real S-parameters of the network can be calculated as

$$\begin{aligned}
S_{11} &= \frac{\left[\left(\frac{S'_{11} - e_{00}}{e_{10}e_{01}} \right) \left(1 + \left(\frac{S'_{22} - e_{33}}{e_{23}e_{32}} \right) e_{22} \right) - \left(\frac{S'_{21} - e_{30}}{e_{10}e_{32}} \right) \left(\frac{S'_{12} - e_{03}}{e_{01}e_{23}} \right) e_{22} \right]}{D} \\
S_{21} &= \frac{\left(\frac{S'_{21} - e_{30}}{e_{10}e_{32}} \right)}{D} \\
S_{22} &= \frac{\left[\left(\frac{S'_{22} - e_{33}}{e_{23}e_{32}} \right) \left(1 + \left(\frac{S'_{11} - e_{00}}{e_{01}e_{10}} \right) e_{11} \right) - \left(\frac{S'_{12} - e_{03}}{e_{01}e_{23}} \right) \left(\frac{S'_{21} - e_{30}}{e_{10}e_{32}} \right) e_{11} \right]}{D} \\
S_{12} &= \frac{\left(\frac{S'_{12} - e_{03}}{e_{01}e_{23}} \right)}{D},
\end{aligned} \tag{6}$$

where

$$\begin{aligned}
D &= \left(1 + \frac{S'_{11} - e_{00}}{e_{10}e_{01}} e_{11} \right) \left(1 + \frac{S'_{22} - e_{33}}{e_{23}e_{32}} e_{22} \right) \\
&\quad - \left(\frac{S'_{21} - e_{30}}{e_{10}e_{32}} \right) \left(\frac{S'_{12} - e_{03}}{e_{01}e_{23}} \right) e_{11}e_{22}.
\end{aligned} \tag{7}$$

Since the calibration algorithm has been determined, the next step is to design the measurement fixture. In our work, the measurement standards are designed firstly. For an ideal thru standard, its impedance should match the standard characteristic impedance of the system. The impedance and electrical length of a microstrip line can be calculated as [4]

$$\begin{aligned}
Z_0 &= \begin{cases} \frac{60}{\sqrt{\epsilon_e}} \ln \left(\frac{8d}{W} + \frac{W}{4d} \right) & \frac{W}{d} \leq 1 \\ \frac{120\pi}{\sqrt{\epsilon_e} [W/d + 1.393 + 0.667 \ln(W/d + 1.444)]} & \frac{W}{d} > 1 \end{cases} \tag{8}
\end{aligned}$$

$$l_e = \frac{l_p f}{c / \sqrt{\epsilon_e}} \times 360^\circ, \tag{9}$$

where

$$\epsilon_e = \frac{\epsilon_r + 1}{2} + \frac{\epsilon_r - 1}{2} \left(1 + \frac{12d}{W} \right)^{-0.5}. \tag{10}$$

c is the speed of electromagnetic waves in vacuum and l_f is the physical length of the microstrip line. In our design, the substrate Taconic TLX-7-0310-C1 with $\epsilon_r = 2.6$, $\tan \delta = 0.0019$, and $h = 0.79$ mm is chosen. Then the line width at 50Ω can be calculated to be 2.14 mm. The length of the thru standard is comparatively flexible. Considering that the reflect standard is only half the length of the thru standard, 2λ (720°) at 12 GHz is chosen, and the physical length can be calculated to be about 35.4 mm. The structure of the thru standard is shown in Figure 2.

As for the reflect standard, the phase of the reflection coefficients of the two ports should be the same. Therefore,

the reflect standard should be symmetrical. In real applications, the reflect standard can be either open-ended or short-ended. But for the open-ended structure, the fringing capacitance cannot be neglected, especially at high frequency range, which can deteriorate the measurement results considerably. So in order to achieve better calibration, the short-ended structure is adopted. The reflect standard is shown in Figure 3. The microstrip lines are half the length of the thru standard and are both connected to a common ground plane in the middle.

Compared with the thru standard, the line standard should have the same characteristic impedance but with a longer phase delay. For measurement accuracy, the phase delay should be controlled between 20° and 160° to avoid phase ambiguity [5, 6]. The electrical length can be calculated using (9). Based on the optimization using the simulation software ADS, when the physical length of the line standard is 6.8 mm longer than the thru standard, the additional phase delays at 2 GHz and 12 GHz are 24.6° and 149.5° , which satisfies the phase delay requirement. Then, the length of the line standard is determined to be 42.2 mm (shown in Figure 4).

The final measurement standard is the match standard. The key to designing a good match standard is to avoid reflection at the ports [7, 8]. Therefore, the impedance of the loads should be strictly matched to the system characteristic impedance. In our design, two pairs of 100Ω chip resistors in parallel position are employed for the loads (shown in Figure 5). The match standard can only be used in lower frequency range due to the high-frequency parasitic effects caused by the resistors. TRM calibration method is applied from 45 MHz to 2 GHz in our design.

SMD components have many different packaging types. The 1210 packaging with length of 2.0 mm, width of 1.25 mm, and height of 0.5 mm is most commonly used. Therefore, in our experiment, the SMD capacitors with 1210 packaging type are measured and analyzed. The structure for measuring SMD components is shown in Figure 6. It is similar to the thru standard except that a slot with the width of 1.5 mm is added in the middle. SMD components can be put across the slot for measurement.

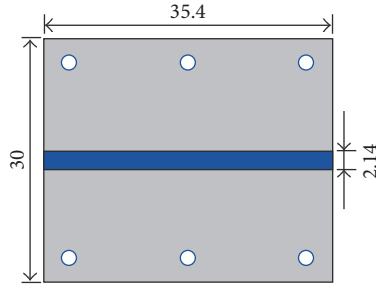


FIGURE 2: The structure of the thru standard.

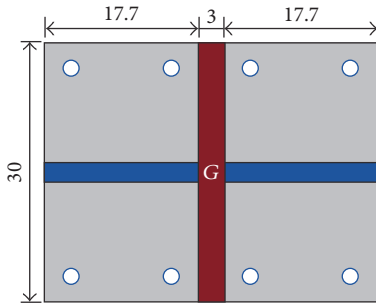


FIGURE 3: The structure of the reflect standard.

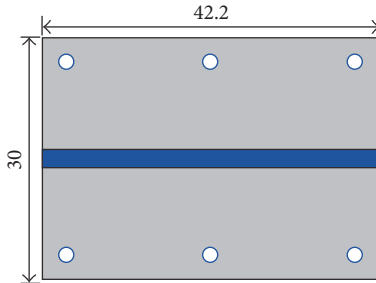


FIGURE 4: The structure of the line standard.

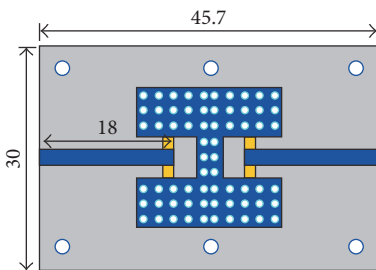


FIGURE 5: The structure of the match standard.

Based on the calibration standards and the measurement structure, the measurement fixture is designed and shown in Figure 7. The leveling screws are used to bring the instrument into level. The base can prevent the structure from tipping over. The movable panel is used to adjust the length so that different measurement standards can fit in. The steel

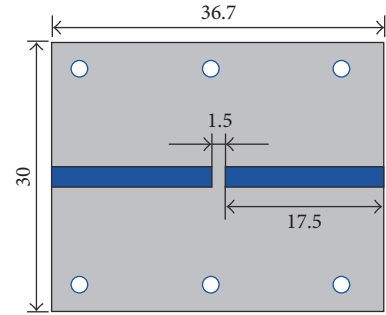


FIGURE 6: The structure for measuring SMD component.

weight is to press down the SMD components for fixing. The measurement fixture is fabricated using stainless steel. The photograph of the measurement equipment is shown in Figure 8.

An SMD capacitor is not an ideal capacitor due to its parasitic effects. The equivalent circuit model of the SMD capacitor is shown in Figure 9. C is the intrinsic capacitance. C_p is the parasitic capacitance caused by the metal wires between the capacitors. There are more than one equivalent model of capacitors in Figure 9, where C_p is parallel with the intrinsic capacitor. L_s and R_s are the inductance and resistance of the metal wires. Therefore, a series resonance can be caused by C and L_s . The frequency can be determined approximately as

$$f_{SR} = \frac{1}{2\pi\sqrt{L_s C}}. \quad (11)$$

When the working frequency exceeds f_{SR} , the capacitor becomes an inductor. So, in real application, SMD capacitors can only be used below their series resonant frequencies. Based on the equivalent circuit model, a parallel resonance can also be produced by C_p and L_s , where the capacitor can be seen to be open-circuited. But C_p generally has a smaller value; the parallel resonant frequency is higher than the series resonant frequency.

The next step is measurement. The measurement is performed using the vector network analyzer HP8510B and the photograph of the measurement setup is shown in Figure 10. The measurement steps are given as follows:

- (1) Calibrate the VNA from 45 MHz to 12 GHz.
- (2) Measure the S-parameters of the thru, reflect, and match standards from 45 MHz to 2 GHz. Measure the S-parameters of the thru, reflect, and line standards from 2 GHz to 12 GHz. Copy the measurement data into a computer.
- (3) Measure the SMD capacitors on the measurement structure. Copy the measurement data into the computer.
- (4) Calculate the corrected data using Matlab based on (2)–(7). Compare these results with the reference results given by Johanson Technology.

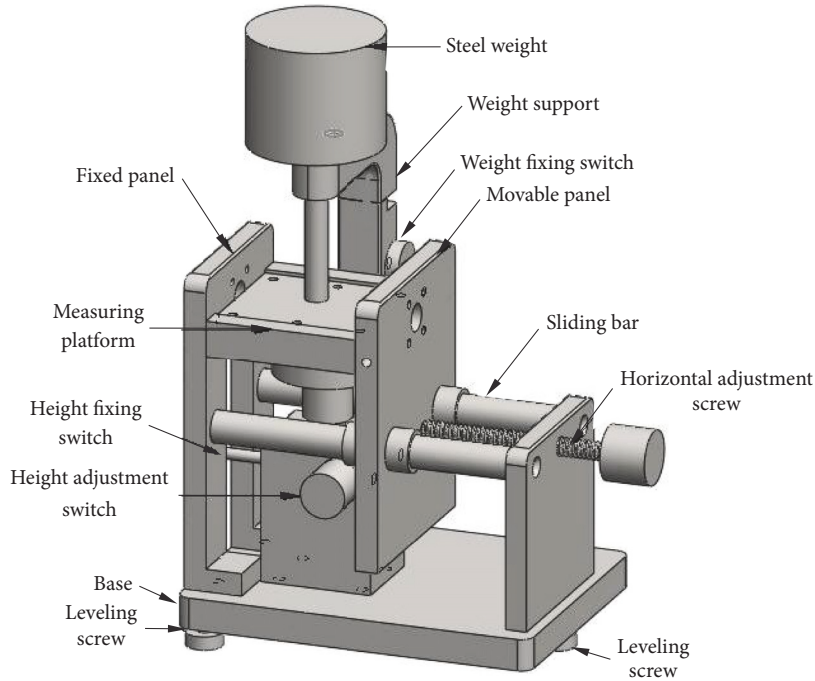


FIGURE 7: The structure of the measurement fixture.

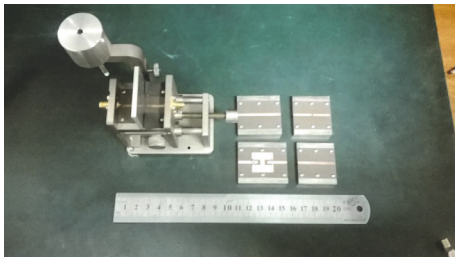


FIGURE 8: The photograph of the designed measurement equipment.

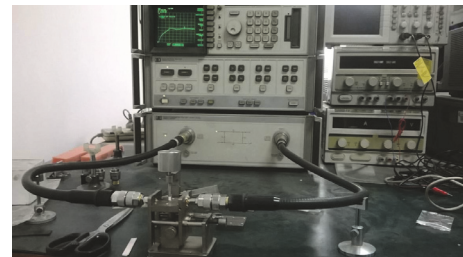


FIGURE 10: The photograph of the measurement setup.

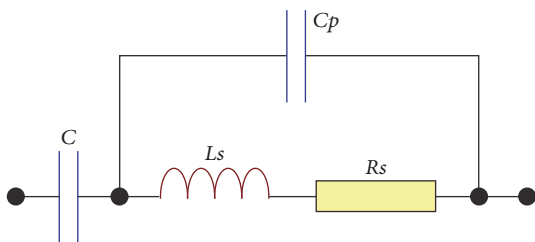


FIGURE 9: The equivalent circuit model for SMD capacitors.

In our experiment, multilayered ceramic SMD capacitors with the values of 2.0, 3.9, 5.6, 8.2, 10, 18, 30, 47, and 100 pF have been measured. Here, we take the 2.0 pF capacitor as an example to show the measurement results. The measured

S-parameters are shown in Figure 11, and the reference S-parameters provided by Johanson Technology are given in Figure 12. By comparison, the measured results are generally in good agreement.

From Figure 11, there is an attenuation point at 8.7 GHz with the insertion loss of 17.4 dB. This is the parallel resonant frequency. Since the value of C_p is comparatively small according to the equivalent circuit, the series resonant frequency point is approximately at 3.45 GHz, where phase $(S_{21}) = 0$. Based on the measured S-parameters, the effective capacitance C_{eff} of the capacitor can be extracted. First, the S-parameters are converted to Y-parameters. And then C_{eff} can be calculated to be $Im(Y_{21})/(j\omega)$. The calculated results are shown in Figure 13. Here, the series resonant point can be clearly observed at 3.45 GHz. When the frequency exceeds the series resonant frequency, the value of C_{eff}

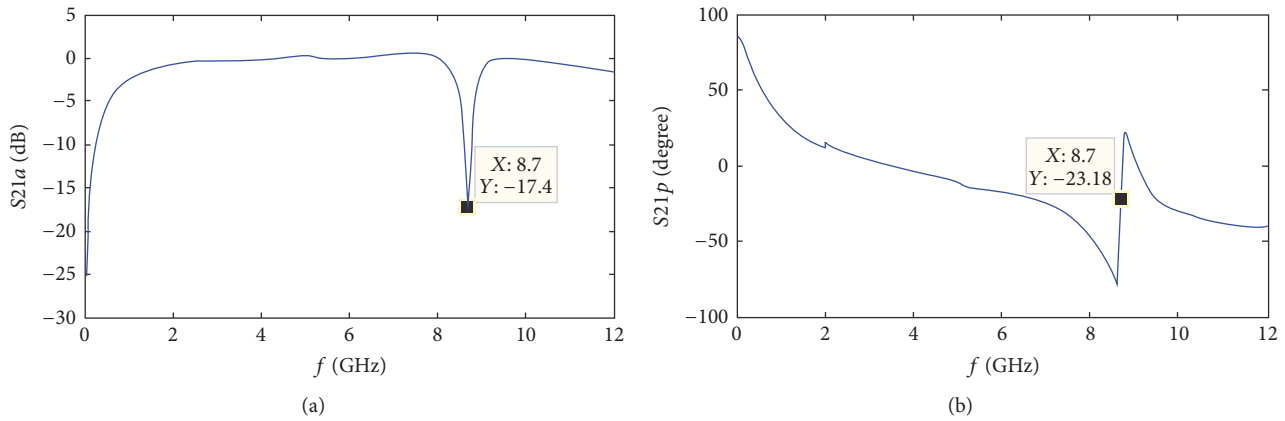


FIGURE 11: The measured S-parameters of the 2.0 pF capacitor: (a) magnitude and (b) phase.

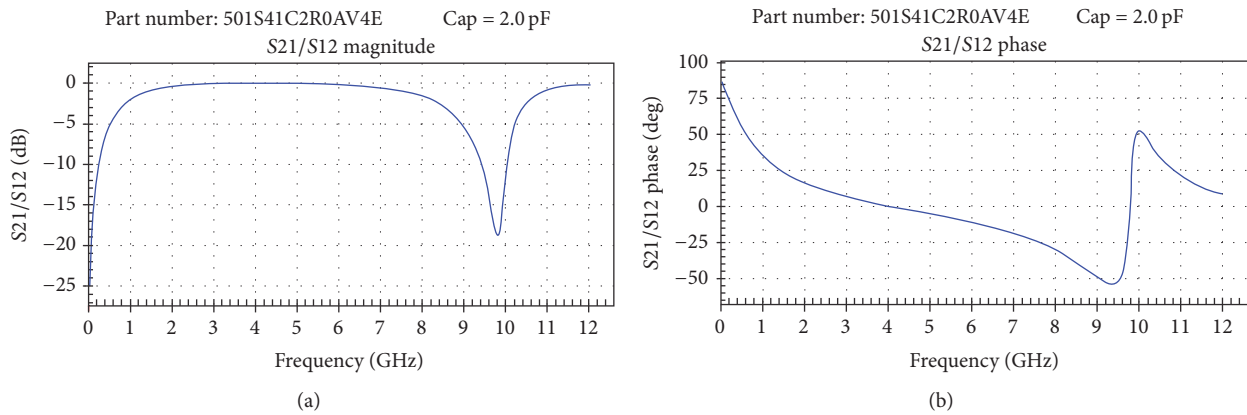


FIGURE 12: The reference S-parameters of the 2.0 pF capacitor provided by Johanson Technology: (a) magnitude and (b) phase.

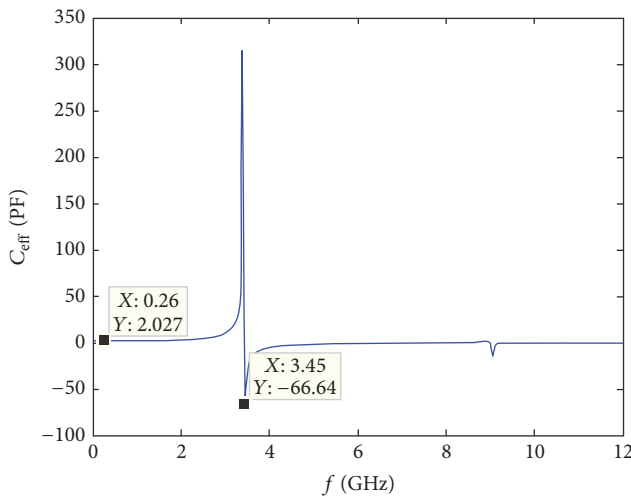


FIGURE 13: The effective capacitance of the capacitor.

becomes negative, which indicates that the capacitor is now in fact an inductor. Therefore, for SMD capacitors, they can only be used under their series resonant frequencies in real applications.

In our experiment, other capacitors with values of 3.9, 5.6, 8.2, 10, 18, 30, 47, and 100 pF are also measured, and the results are shown in Figure 14. The measured capacitance values are in good agreement with the reference values. It can also be observed that, with the increase of the capacitance value, the series resonant frequency decreases. This indicates that SMD capacitors with larger capacitance can only be applied in lower frequency ranges. In general, satisfactory results have been achieved.

3. Conclusion

In this paper, a wide-band test fixture is designed for the measurement of parasitic effects of RF passive SMD components. Two calibration methods (TRM and TRL) are used. Good results have been achieved. The proposed test fixture can be applied to measure SMD components from VHF band up to X band.

Conflicts of Interest

The authors declare that there are no conflicts of interest regarding the publication of this paper.

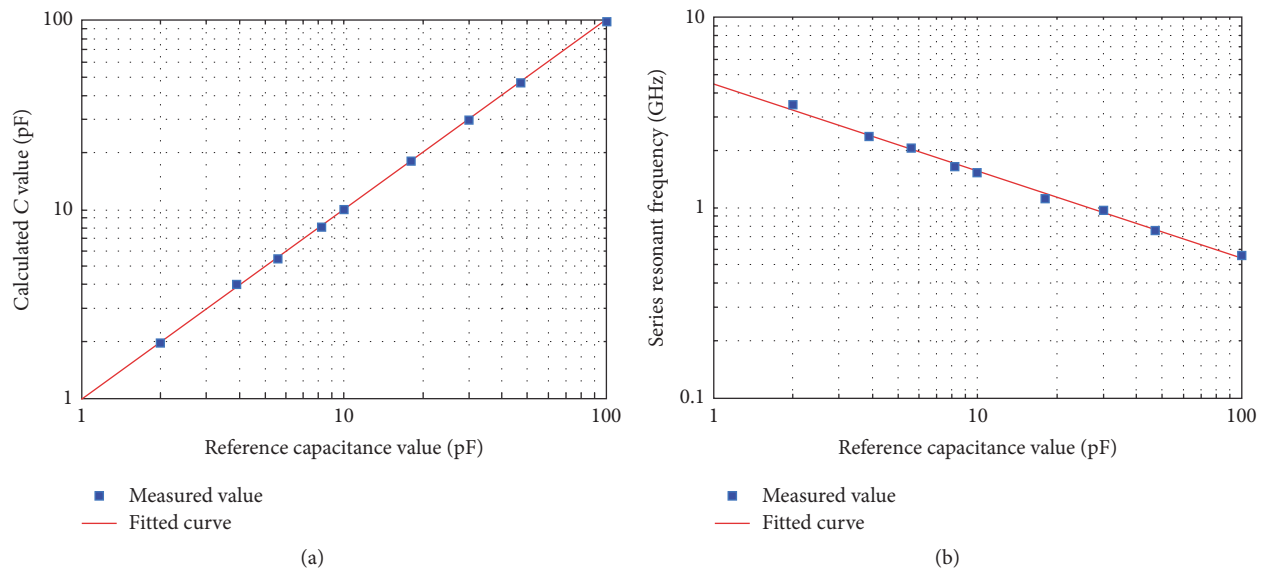


FIGURE 14: The measured results of other capacitors.

Acknowledgments

This work is supported by the National Natural Science Foundation of China (Grant nos. 61301022 and U1430102).

References

- [1] V. Teppati, A. Ferrero, and S. Mohamed, *Modern RF and Microwave Measurement Techniques*, Cambridge University Press, 2013.
- [2] N. Borges Carvalho and S. Dominique, *Microwave and Wireless Measurement Techniques*, Cambridge University Press, 1st edition, 2013.
- [3] J. P. Dunsmore, *Handbook of Microwave Component Measurements: with Advanced VNA Techniques*, Wiley, 1st edition, 2012.
- [4] D. M. Pozar, *Microwave Engineering*, Wiley, 4th edition, 2011.
- [5] Y. Liu, L. Tong, Y. Tian et al., "Measurements of planar microwave circuits using an improved TRL calibration method," *Progress in Electromagnetics Research*, vol. 109, pp. 263–278, 2010.
- [6] U. Stumper, "Influence of nonideal LRL or TRL calibration elements on VNA S-parameter measurements," *Advances in Radio Science*, vol. 3, pp. 51–58, 2005.
- [7] E. Centeno-Calero Clara, "Design of a TRM calibration Kit for the ZMA coaxial interface using ansoft HFSS," *Microwave Journal*, vol. 46, no. 6, pp. 88–101, 2003.
- [8] Pulido-Gaytan., M. Alejandro, Reynoso-Hernandez. et al., "Generalized theory of the thru-reflect-match calibration technique," *IEEE Transaction on Microwave Theory and Techniques*, vol. 63, no. 5, pp. 1693–1699, 2015.



Hindawi

Submit your manuscripts at
<https://www.hindawi.com>

